Mon. Not. R. Astron. Soc. **000**, 000–000 (0000) Printed 4 May 2011 (MN LATEX style file v2.2)

Clues to the "Magellanic Galaxy" from Cosmological Simulations

Laura V. Sales[1], Julio F. Navarro,[2] Andrew P. Cooper[1,3] Simon D. M. White[1], Carlos S. Frenk[3] and Amina Helmi[4]

[1] *Max Planck Institute for Astrophysics, Karl-Schwarzschild-Strasse 1, 85740 Garching, Germany*
[2] *Department of Physics and Astronomy, University of Victoria, Victoria, BC V8P 5C2, Canada*
[3] *Department of Physics, Institute for Computational Cosmology, University of Durham, South Road, Durham DH1 3LE*
[4] *Kapteyn Astronomical Institute, University of Groningen, PO Box 800, 9700 AV Groningen, the Netherlands*

4 May 2011

ABSTRACT

We use cosmological simulations from the Aquarius Project to study the orbital history of the Large Magellanic Cloud (LMC) and its potential association with other satellites of the Milky Way (MW). We search for dynamical analogs to the LMC and find a subhalo that matches the LMC position and velocity at either of its two most recent pericentric passages. This suggests that the LMC is not necessarily on its first approach to the MW, provided that the virial mass of the Milky Way is as high as that of the parent Aquarius halo; $M_{200} = 1.8 \times 10^{12}\, M_{\odot}$. The simulation results yield specific predictions for the position and velocity of systems associated with the LMC prior to infall. If on first approach, most should lie close to the LMC because the Galactic tidal field has not yet had enough time to disperse them. If on second approach, the list of potential associates increases substantially, because of the greater sky footprint and velocity range of LMC-associated debris. Interestingly, our analysis rules out an LMC association for Draco and Ursa Minor, two of the dwarf spheroidals suggested by Lynden-Bell & Lynden-Bell to form part of the "Magellanic Ghostly Stream". Our results also indicate that the direction of the orbital angular momentum is a powerful test of LMC association. This test, however, requires precise proper motions, which are unavailable for most MW satellites. Of the 4 satellites with published proper motions, only the Small Magellanic Cloud is clearly associated with the LMC. Taken at face value, the proper motions of Carina, Fornax and Sculptor rule them out as potential associates, but this conclusion should be revisited when better data become available. The dearth of satellites clearly associated with the Clouds might be solved by wide-field imaging surveys that target its surroundings, a region that may prove a fertile hunting ground for faint, previously unnoticed MW satellites.

Key words: galaxies: haloes - galaxies: formation - galaxies: evolution - galaxies: kinematics and dynamics.

1 INTRODUCTION

The Large and Small Magellanic Clouds (LMC and SMC, respectively) are unusual satellite galaxies. They are exceptionally bright, and so close to the Milky Way (MW) that recent studies have concluded that fewer than one in ten MW-like systems are expected to host satellites with properties similar to the Clouds (Boylan-Kolchin et al. 2010; Busha et al. 2010; Liu et al. 2010; Guo et al. 2011). The short crossing time at their present Galactocentric distance suggests that they may have already completed a number of orbits in the Galactic potential (Murai & Fujimoto 1980; Lin & Lynden-Bell 1982; Gardiner et al. 1994; van der Marel et al. 2002) while their proximity suggests that they form a bound pair.

If the LMC/SMC are truly physically associated, then it is likely that they were once part of a larger system: the "Greater Magellanic Galaxy", to quote Lynden-Bell (1982). This idea has prompted searches for evidence that other satellites might have been in the past associated with the Clouds. This is encouraged, in part, by the "polar" distribution of the brightest Galactic satellites, which seems to trace the orbital path of the Clouds (Lynden-Bell 1976). Lynden-Bell & Lynden-Bell (1995), for example, suggested a possible association between the LMC, SMC, Draco, Ursa Minor, Carina and Sculptor as part of a common "Ghostly Stream".

The association between different satellites has recently received renewed attention, motivated mainly by coherence in the position and velocities of satellite pairs such as Leo IV and Leo V (Belokurov et al. 2008)) and of satellites near the Sagittarius stream; e.g., Segue 1 (Niederste-Ostholt et al. 2009), Bootes II (Koch et al. 2009), and Segue 2 (Belokurov et al. 2009). These ideas have received support from the realization that most satel-

lites should have been accreted into the Milky Way as part of multiple systems and have gained momentum because testing the predictions of such scenario has become possible using realistic cosmological simulations (Sales et al. 2007a; Li & Helmi 2008; D'Onghia & Lake 2008; Ludlow et al. 2009; Klimentowski et al. 2010).

The Magellanic Clouds are also unusual in their kinematics. The latest proper motion measurements of stars in the Large Magellanic Cloud (Kallivayalil et al. 2006; Piatek et al. 2008) indicate that the LMC has a much higher tangential velocity than previously thought ($V_t \sim 370$ km/s), raising questions as to whether the LMC and SMC are actually bound to each other or even to the Galaxy as a whole. Besla et al. (2007), for example, have used the new kinematic data to revise earlier orbital models (see, e.g., van der Marel et al. 2002) and concluded that the LMC and SMC must be on the first pericentric passage of their orbit around the Milky Way if the MW virial mass is of the order of $\sim 10^{12}\,M_\odot$, as argued by Klypin et al. (2002).

The discussion above depends sensitively on the assumed virial mass of the Galaxy. Bright satellites are more common around more massive primaries (Guo et al. 2011), and higher primary masses make it easier to accommodate high orbital speeds for the satellites. Even a factor of two increase in virial mass can make a difference (Piatek et al. 2008; Shattow & Loeb 2009), which is certainly within the current uncertainty in virial mass estimates for the Milky Way (Battaglia et al. 2005; Smith & et al. 2007; Sales et al. 2007b; Li & White 2008; Xue et al. 2008; Reid et al. 2009; Gnedin et al. 2010).

The escape speed at $r = 50$ kpc from a Navarro-Frenk-White halo with virial mass[1] $M_{200} = 2 \times 10^{12}\,M_\odot$ is of order ~ 500 km/s, which would mean that the Clouds are safely bound to the Galaxy despite their high speed. Further, Besla et al. (2007) show that virial masses as high as that imply a radial period of just about 3 Gyr and hence the possibility that the LMC and SMC have completed multiple orbits around the Galaxy. A first infall scenario is, on the other hand, compelling for a number of reasons, including the recent successful modeling of the Magellanic Stream as a tidal relic of a recent interaction between the clouds before infall into the Milky Way (Besla et al. 2010).

The discussion above highlights the fact that basic issues such as whether the LMC and SMC are on their first approach, or bound to each other, or truly associated with other MW satellites, remain unresolved. These questions are clearly interrelated. For example, the relative positions and velocities of satellites of past LMC associates would be very different if the Clouds are on first or second approach. Careful modeling is therefore required to interpret current data, especially because the orbit of the Clouds should be eroded quickly by dynamical friction and by tidal mass loss, limiting the applicability of models such as that of Besla et al. (2007), which assume that the Clouds evolve in a rigid Galactic potential.

We address these issues here by using the Aquarius Project, a series of cosmological simulations of the formation of a Milky Way-sized halo in the LCDM paradigm (Springel et al. 2008). Because of their extraordinary numerical resolution, we are able to trace the orbits not only of massive subhalos, but also of subhalos within subhalos, thus enabling a realistic assessment of their orbital paths before, during, and after their accretion into the Milky Way halo.

This paper is organized as follows. In Sec. 2 we provide a brief description of the Aquarius simulations. We analyze the orbit of an LMC candidate in Sec. 3.1, and the spatial and kinematic properties of their associated subhalos in Sec. 3.2. We use these results to explore in Sec. 3.3 which satellites of the Milky Way might have been associated with the Clouds in the past. Sec. 4 summarizes our main conclusions.

2 THE NUMERICAL SIMULATIONS

2.1 The Aquarius Project

The Aquarius Project (Springel et al. 2008) is a series of cosmological simulations of the formation of six dark matter halos with mass consistent with that expected for the halo of the Milky Way. The simulations assume the ΛCDM cosmology, with parameters chosen to match the WMAP 1-year data (Spergel et al. 2003): matter density parameter, $\Omega_{\rm M} = 0.25$; cosmological constant term, $\Omega_\Lambda = 0.75$; power spectrum normalization, $\sigma_8 = 0.9$; spectral slope, $n_s = 1$; and Hubble parameter, $h = 0.73$.

The halos were identified in a large N-body simulation of a cube 137 ($100\,h^{-1}$) Mpc comoving on a side, a lower resolution version of the Millennium-II Simulation (Boylan-Kolchin et al. 2009). This volume was resimulated using the same power spectrum and phases of the original simulation, but with additional high-frequency waves added to regions encompassing the initial Lagrangian volume of each halo. The high-resolution region was populated with low-mass particles and the rest of the volume with particles of higher mass (Power et al. 2003).

The six Aquarius halos are labelled "Aq-A" through "Aq-F". Each was resimulated at different resolutions in order to assess numerical convergence. A suffix, 1 to 5, identifies the resolution level, with level 1 denoting the highest resolution. Between levels 1 and 5, the particle mass ranges from $m_p = 2 \times 10^3\,M_\odot$ to $= 3 \times 10^6 M_\odot$. At $z = 0$, the six halos have similar "virial" mass, roughly between 1 and $2 \times 10^{12} M_\odot$. For further details of the Aquarius Project, we refer the reader to Springel et al. (2008) and Navarro et al. (2010).

2.2 Identification of the LMC analog

We search the Aquarius simulations for accretion events that result in systems with kinematics similar to that of the LMC. In particular, we look for relatively massive systems (i.e., with masses exceeding 1% of the main halo mass) that are accreted relatively recently (i.e., after $z = 1$), and that have, at pericenter, distances and velocities of order 50 kpc and 400 km/s, respectively.

Our best candidate is a system that accretes into the main Aq-A halo at $z = 0.51$ ($t = 8.6$ Gyr, i.e., ~ 5 Gyr before the present time). Just before accretion, at $z_{\rm id} = 0.9$ ($t_{\rm id} = 6.6$ Gyrs), this subhalo has a virial mass of $M_{200} = 3.6 \times 10^{10} M_\odot$. Our analysis below focuses on this "LMC-analog" halo and its substructures associated to the same friends-of-friends group ("LMCa group", for short) in the Aq-A-3 simulation. This level-3 simulation has a particle mass $m_p = 4.9 \times 10^4 M_\odot$, and therefore LMCa is resolved with more than $700,000$ particles. SUBFIND (Springel et al. 2001) is used to identify self-bound substructures within LMCa; at $t_{\rm id}$

[1] The virial mass, M_{200}, is defined as the mass contained within r_{200}, the radius of a sphere of mean density 200 times the critical density for closure, $\rho_{\rm crit} = 3H^2/8\pi G$. This choice defines implicitly the virial radius of the halo, r_{200}, and its virial velocity, V_{200}.

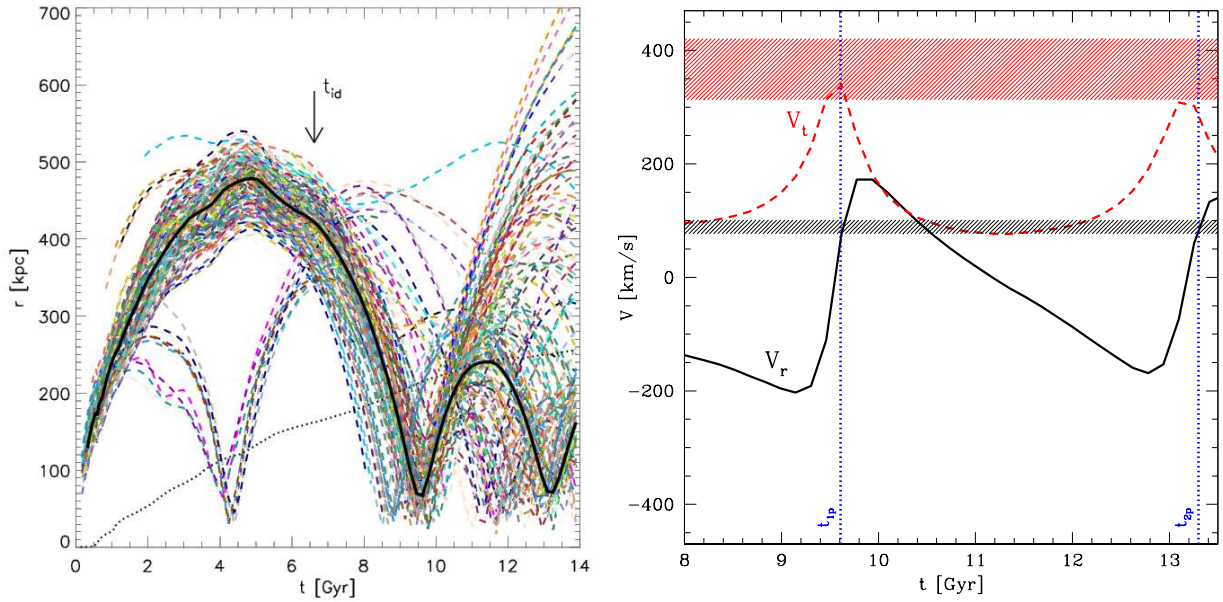

Figure 1. *Left panel:* Time evolution of the galactocentric distance of the "LMC-analog" (LMCa) halo (solid black curve) as well as that of its subhalos (dashed curves), identified at $t_{\rm id}$ (vertical arrow). Note the complex orbital evolution of associated subhalos, which include a few that are temporarily captured by LMCa after being "ejected" from the main halo during the tidal dissociation of a group accreted at $t \sim 4$ Gyr. The LMC analog enters the virial radius of the main halo (marked by the dotted line) at $t \sim 9$ Gyr and reaches its first pericenter at $t \sim 9.6$ Gyr. After first pericenter the subhalo loses 38% of its mass and its orbital apocenter is reduced to ~ 250 kpc, about half of its first turnaround distance. A non-negligible fraction of subhalos ($\sim 4\%$) are ejected into very eccentric orbits after first pericenter, whereas others settle onto more bound orbits with shorter periods. The main subhalo reaches its second pericenter at $t \sim 13.3$ Gyr still surrounded by some of its most bound companions. *Right panel:* Radial and tangential velocity of the main subhalo as a function of time. Shaded areas correspond to the observed velocity of the LMC ($\pm 3\sigma$) based on the proper motion measurements of Kallivayalil et al. (2006). Blue dotted vertical lines indicate the times t_{1p} and t_{2p} (near first and second pericenter passages) when the kinematics of LMCa best matches that of the LMC.

there are more than 250 LMCa subhalos with masses exceeding $1 \times 10^6 M_\odot$.

As may be seen from Fig. 1, the LMCa group turns around at $t_{\rm ta} = 5$ Gyr ($z = 1.3$) from a distance of $r_{\rm ta} = 480$ kpc (all distances and velocities quoted are physical unless explicitly stated otherwise). LMCa reaches its first pericenter at $t_{\rm per1} = 9.5$ Gyr, with pericentric distance ($r_{\rm per1} = 63$ kpc) and speed ($V_{\rm per1} = 355$ km/s) comparable to those of the LMC. The LMCa orbit becomes substantially more bound after first pericenter due to dynamical friction and tidal mass loss, so that it reaches a distance of only 240 kpc at its second apocenter, at $t = 11.5$ Gyr. Its radial period reduced to 3.8 Gyr, it goes through pericenter again at $t_{\rm per2} = 13.3$ Gyr, with similar pericentric distance and speed as the first (see right panel of Fig. 1).

The best match to the kinematic properties of the LMC occurs just after each of these pericentric passages, at times that we will denote t_{1p} and t_{2p}. These are shown in the right panel of Fig. 1 with vertical dotted lines. At these times, the virial mass of the host halo is 1.6 and $1.8 \times 10^{12}\ M_\odot$, respectively. At $t = t_{1p}(t_{2p})$, the satellite is at a distance of $65(69)$ kpc, with radial velocity $V_r = 78(89)$ km/s and tangential velocity $V_t = 347(300)$ km/s. In the analysis that follows we focus on the properties of LMCa and its associated subhalos at t_{1p} and t_{2p}.

3 RESULTS

3.1 The Orbit of the LMCa Group

The left panel of Fig. 1 shows the radial evolution of LMCa and its 250 most massive associated subhalos (identified at $t_{\rm id}$ within the same friends-of-friends group). This shows the complex orbital behaviour of LMCa subhalos as the group gets disrupted in the tidal field of the primary halo. As emphasized by Sales et al. (2007a) and Ludlow et al. (2009), many satellites undergo drastic changes in energy and angular momentum during pericentric passage, causing some systems to achieve escape velocity and to leave the primary halo altogether.

Interestingly, the LMCa group itself contains captured "escapees" from another group. As may be seen in the left panel of Fig. 1, a number of subhalos belonging to LMCa at $t_{\rm id}$ were actually accreted much earlier into the main halo and ejected from it when their parent group was disrupted at $t \sim 4$ Gyr. By chance these were then temporarily captured by LMCa at $t_{\rm id}$ before plunging again into the main halo.

These changes limit the applicability of the usual procedure of looking for satellite associations by searching for objects of common energy and/or angular momentum (see, e.g., Lynden-Bell & Lynden-Bell 1995). Instead of making simple assumptions we shall use directly the 6D information from the simulations to assess the probability that other Milky Way satellites are associated with the LMC.

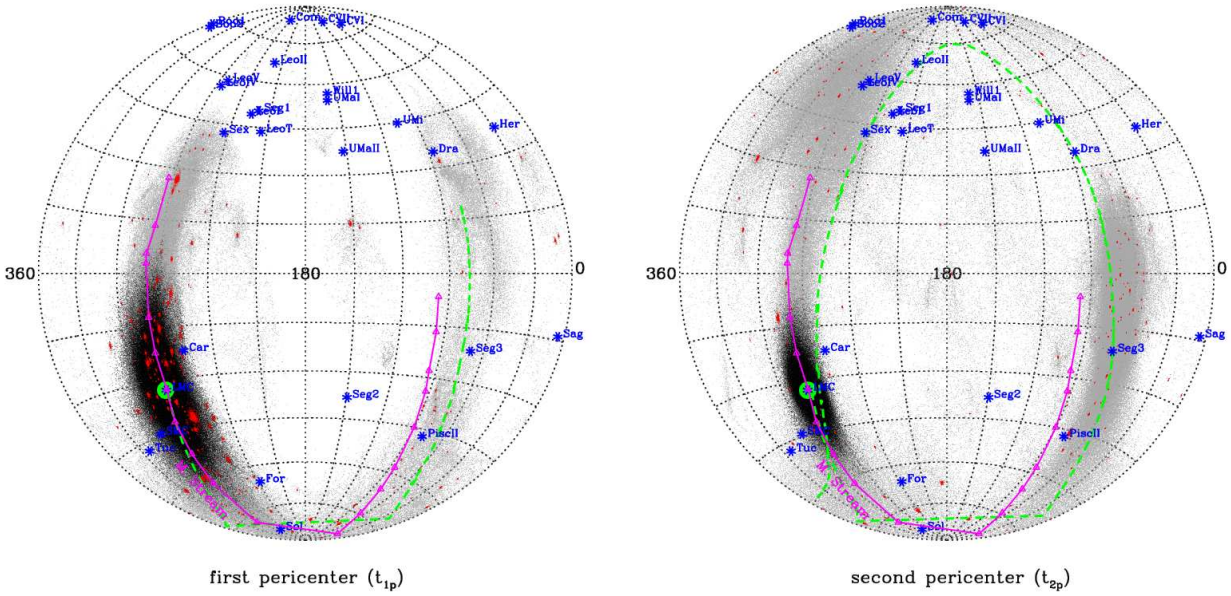

Figure 2. Aitoff projection of all particles belonging to the LMCa group at two different times, t_{1p} (near 1st pericenter, left panel) and t_{2p} (near 2nd pericenter, right panel), when the kinematics of the most massive LMCa member (shown by a green circle) matches best that of the Large Magellanic Cloud (see Fig. 1). Dots denote all individual particles within the virial radius of the LMCa at the time of identification, $t_{\rm id}$. Those colored black are still bound to LMCa; grey are those that have become unbound as a result of the tidal interaction with the primary halo. Particles in red are those belonging to self-bound substructures of LMCa. The positions in the sky of all known Milky Way satellites are also shown and labelled in blue. The orbital path of LMCa is shown by the dashed green curve; a magenta curve traces the location of the Magellanic Stream, taken from Nidever et al. (2010). The reference frame of the simulation has been rotated so that the position in the sky and the proper motion of LMCa match those of the LMC. Note how all particles and substructures associated with LMCa stretch along the orbital path. At t_{1p} (panel on the left) most associated subhalos lie near the LMC since tidal stripping has not yet had enough time to disrupt the system. At t_{2p} (panel on the right) the particles and subhalos associated with LMCa are more widely spread across the sky but still trace the orbital path. The LMCa footprint can be used, together with velocity information, to investigate whether other Milky Way satellites have been associated with the LMC in the past. See text for further details.

3.2 Position and Kinematics of the LMCa Group

We plot in Fig. 2 the position in the sky (in an Aitoff projection) of all particles identified at $t_{\rm id}$ to belong to LMCa. The panel on the left corresponds to first pericenter, t_{1p}, and that on the right to second pericenter, t_{2p}. The simulation reference frame has been rotated so that the position in the sky and the direction of motion of the main LMCa subhalo (indicated by a green circle) coincide with those of the LMC. The orbital path is shown by a green dashed line; the line in magenta traces the Magellanic Stream (Nidever et al. 2010). Particles in black are those currently still bound to LMCa, those in grey correspond to tidally stripped LMCa material. Particles in red highlight the LMCa substructures that remain self-bound.

Fig. 2 shows the complex footprint on the sky traced by LMCa and its debris, and how it changes substantially from first to second pericentric passage. At first approach (left panel of Fig. 2), most LMCa subhalos cluster around the LMC because tidal stripping has not yet had enough time to disrupt the system. Nevertheless, there are a few tidally-stripped systems (those more loosely bound to LMCa at $t_{\rm id}$), and they roughly trace the orbit of LMCa along a nearly polar circle. The sky is not uniformly populated by the stream; for example, because the pericentric passage occurs near the Southern Galactic Pole very few LMCa subhalos have a chance of reaching the northern Galactic cap by t_{1p}. Some systems stray from the orbital plane despite their previous association, but these cases are rare and correspond to subhalos populating the outskirts of the LMCa group at $t_{\rm id}$.

The orbital path is still discernible in the tidal stream at second pericenter, but the debris populates now both hemispheres in the sky. At this time LMCa has lost more than 70% of its original mass to tides, compared with only 40% at $t = t_{1p}$. The distribution of the debrie on the sky would certainly be wider for a progenitor of larger mass than the one considered here

Blue asterisks in Fig. 2 indicate the position of all known Milky Way satellites, including the ultra-faint dwarfs discovered by SDSS, which are located mainly in the northern Galactic cap. Several dwarfs lie along the debris path and therefore could potentially have been associated with the LMC. These include, at $t = t_{1p}$, Sextans (Sex), Draco (Dra), Segue 3 (Seg3), Pisces II (PiscII), Sculptor (Scl), Fornax (For), Tucana (Tuc), Carina (Car), Leo II, and the SMC. Because the debris is more spread out at t_{2p}, the list includes then further dwarfs, such as those in the constellation of Leo.

Of course, true association requires not only coincidence with the LMCa tidal stream in projection, but also in distance and velocity. We investigate this in Fig. 3, where we plot the Galactocentric distance and radial velocity of LMCa particles for $t = t_{1p}$ (left) and $t = t_{2p}$ (right). Color coding is the same as in Fig. 2. Data for all known Milky Way satellites are also shown in each panel, for comparison. Since the LMCa debris is confined to specific regions in the (r, V_r) plane, these data may be used to test the association of any individual dwarf with the LMC, subject to assuming that the

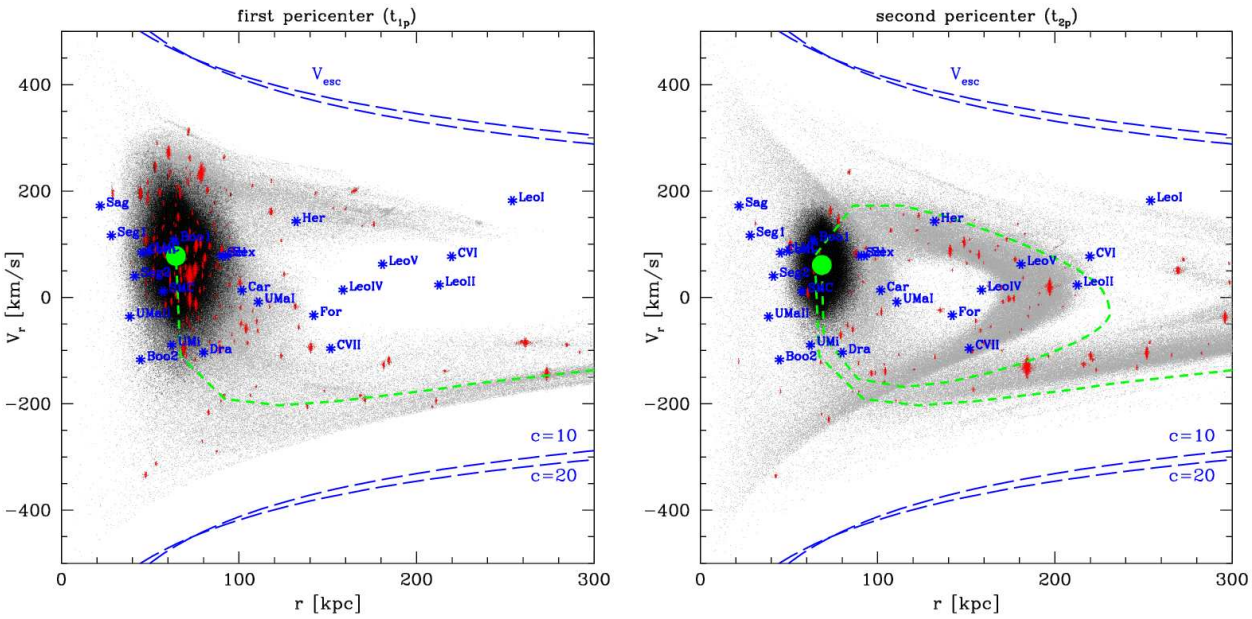

Figure 3. Galactocentric distance versus radial velocity for all particles in the LMCa group, compared with those of known Milky Way dwarfs. Color coding is the same as in Fig. 2. Left and right panels correspond to $t = t_{1p}$ and $t = t_{2p}$, respectively. For reference, the local escape velocity of a Navarro-Frenk-White halo (Navarro et al. 1996, 1997) is indicated by the blue long-dashed curves, for two values of the concentration, $c = 10$ and 20. Note that the tidal debris from LMCa is constrained to a well defined region in the (r, V_r) plane, a fact that may be used to gauge the likelihood of association with the LMC of individual dwarfs.

LMC is either on its first or second approach to the Galaxy. We explore these associations next.

3.3 Association with the Clouds

To be deemed an "LMC associate" a satellite must satisfy at least the following three conditions: (i) it should fall in the celestial sphere within the footprint of the LMCa group; (ii) it should be at a Galactocentric distance consistent with that of LMCa particles at the same location in the sky; and (iii) it should have Galactocentric radial velocity also consistent with LMCa in the same region. In principle a further condition involving the tangential velocity could be added to the list, but the preliminary nature of most proper motion estimates for Milky Way satellites implies the results are unlikely to be conclusive at this stage. We discuss this further below.

3.3.1 Sky proximity

We can quantify the proximity in the sky of any dwarf to the LMCa stream by computing the angular distance to the $n^{\rm th}$ nearest LMCa particle in projection and comparing that with the probability of obtaining a similar distance (or smaller) for a random point in the sky. The histograms in Fig. 4 show the distribution of the angular distance to the 50th nearest LMCa particle, δ_{50}, computed for 10,000 random points in the celestial sphere; the median of the distribution is at $\delta_{\rm lim} = 4^\circ$ and $\delta_{\rm lim} = 2^\circ$ for the first and second pericenter passages, respectively. As may be seen from the inserts in Fig. 4 the footprint of the LMCa stream is traced faithfully by regions satisfying $\delta_{50} < \delta_{\rm lim}$ (shown in red) and we shall use this condition to decide which dwarfs are likely to be associated with the LMC.

According to Fig. 4, at first pericenter only 8 dwarfs satisfy the proximity condition specified above but, because the LMCa footprint covers a much larger fraction of the sky at second pericenter, 17 dwarfs pass this constraint then. These numbers are reasonably insensitive to our choice of n=50, especially at first pericenter; choosing the 100th nearest neighbour results in 9 likely-associated dwarfs at t_{1p} and 22 at t_{2p}.

3.3.2 Radial velocity

Figs. 5 and 6 are then used to check which of these candidate dwarfs are also associated with the stream in distance and velocity. The various panels in these figures show the Galactocentric distance and radial velocity of each of the dwarfs in the LMCa sky footprint, together with those of all LMCa particles closer than $\delta_{\rm lim}$ in the sky from each dwarf. This enables an intuitive test of which satellites have distances and velocities consistent with LMC association.

For example, the top left panel of Fig. 5 corresponds to the SMC and it shows that there are plenty of LMCa particles with distances and radial velocities coincident with the SMC at first approach, endorsing a true association between the LMC and the SMC. An opposite example is provided by Draco; the data in Fig. 5 show that, although it is within the LMCa footprint, all of the particles associated with LMCa at Draco's location have discrepant velocities and/or distances. This is because Draco is projected onto the trailing stream at first pericenter, and one would expect then very large negative radial velocities at Draco's Galactocentric distance. A similar analysis may be carried out for each dwarf individually, but it should be clear from Fig. 5 that, aside from the SMC, only Carina and Fornax seem to have a reasonable chance of being associated with the Clouds if they are on first approach.

The situation is less clear-cut at second pericenter, because the

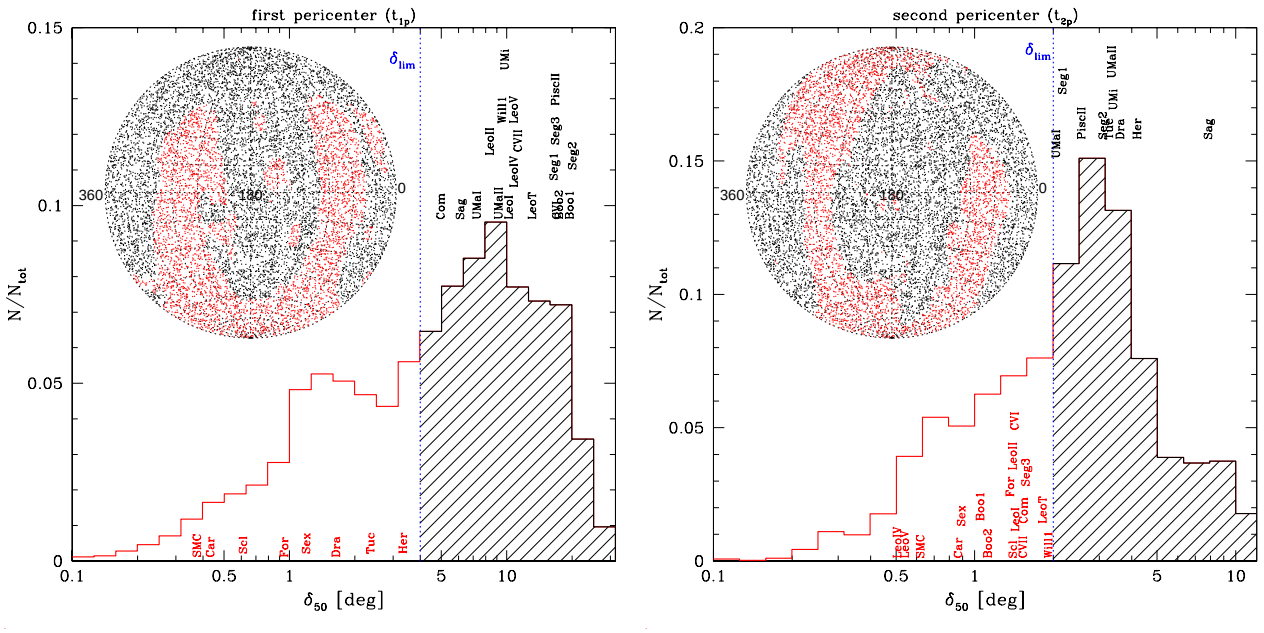

Figure 4. Distribution function of δ_{50}, the angular size (radius) of the circle that contains the 50 nearest LMCa particles in projection, computed for $10,000$ random points in the celestial sphere. Left and right panels correspond to $t = t_{1p}$ and $t = t_{2p}$, respectively. δ_{50} is a useful measure of proximity to the LMCa stream in the sky for any given point. In the inserted Aitoff maps, red is used to highlight points with $\delta_{50} < \delta_{\rm lim}$, where $\delta_{\rm lim}$ is the median of the random distribution. Black points correspond to $\delta_{50} > \delta_{\rm lim}$. As demonstrated by the Aitoff inserts, δ_{50} is a useful measure of association with the stream. We show in each panel the values of δ_{50} corresponding to each Milky Way dwarf, and retain only those with $\delta_{50} < \delta_{\rm lim}$ as potentially associated with the LMC.

LMCa footprint is larger, and because the stream now has multiple wraps, which allows for a wider range of velocities in a given direction in the sky to be consistent with LMCa association. The right panel of Fig. 4 indicates that 17 dwarfs pass the sky proximity test; these are shown (two per panel except in the middle left) in Fig. 6. Inspection of each panel shows that, aside from the SMC, Carina, Canes Venatici II, Sculptor, Leo II, Leo IV, and Leo V could in principle be associated with the LMC. The situation of Fornax, Canes Venatici I, and Sextans is less clear but one would be hard pressed to rule out an association in such cases. Bootes (1 and 2), Segue 3, LeoT, Willman I and Coma are all unlikely to be associated with the LMC.

3.3.3 Orbital angular momentum

The sky proximity and radial velocity constraints discussed above are sensitive to the fact that we consider here a single LMC look-alike system. This is compounded by the relatively low mass of LMCa, compared with the $1.3 \times 10^{11} M_\odot$ suggested by the abundance-matching analysis of Boylan-Kolchin et al. (2010). A more massive subhalo may leave a broader footprint on the sky and lead to a wider range of radial velocities consistent with LMC-associated debris. More conclusive statements about the likelihood of association of the candidate satellites identified in the previous subsections require accurate measurements of the proper motion in order to constrain their tangential velocity and to verify that they follow orbits roughly aligned with the orbital plane of the LMC. Indeed, as we show below, the direction of the orbital angular momentum of a dwarf might be one of the cleanest tests of association with the Clouds.

This is shown in Fig. 7, where we show, in an Aitoff projection, the direction of the orbital angular momentum of LMCa and its associated substructures at first and second pericentric passage. Because of the nearly polar orbit the direction of the angular momentum of most LMCa-associated material is roughly on the Galactic plane, pointing in the direction of the Sun from the Galactic center; i.e., $l = 180^\circ$, $b = 0^\circ$. This tight alignment is preserved at second approach, albeit with larger scatter.

In Galactocentric Cartesian coordinates, with the X-axis pointing away from the Sun, Y-axis defined positive in the direction of Galactic rotation, and positive Z-axis in the direction of the Galactic North Pole, this implies that the X-component of the orbital angular momentum (j_X) of associated satellites should be negative and much larger in magnitude than j_Y or j_Z. This may be seen in Table 1, which lists the components of the *unit* vector identifying the direction of the (average) angular momentum of particles associated in the sky with the candidate dwarfs identified in the previous subsection. Note that, with no exception, the angular momentum points clearly toward $-X$, the anti-Galactic center direction.

This result makes strong predictions regarding the tangential velocity of the candidate satellites, which can be checked against observation for the few satellites with available proper motions (SMC: Kallivayalil (2006b), Carina: Piatek et al. (2003), Fornax: Piatek et al. (2007) and Sculptor: Piatek et al. (2006)). Inspection of Table 1 and Fig. 7 shows that, of the four satellites with published spatial velocities, only the SMC appears associated with the LMC. None of the other three (Carina, Fornax, and Sculptor) seems obviously associated with the Clouds according to this test. We hasten to add, however, that, as the recent revision to the proper motion of the LMC illustrates (Kallivayalil et al. 2006), proper motion measurements are exceedingly difficult, and hence our conclusion should be revisited when new, more accurate data become available.

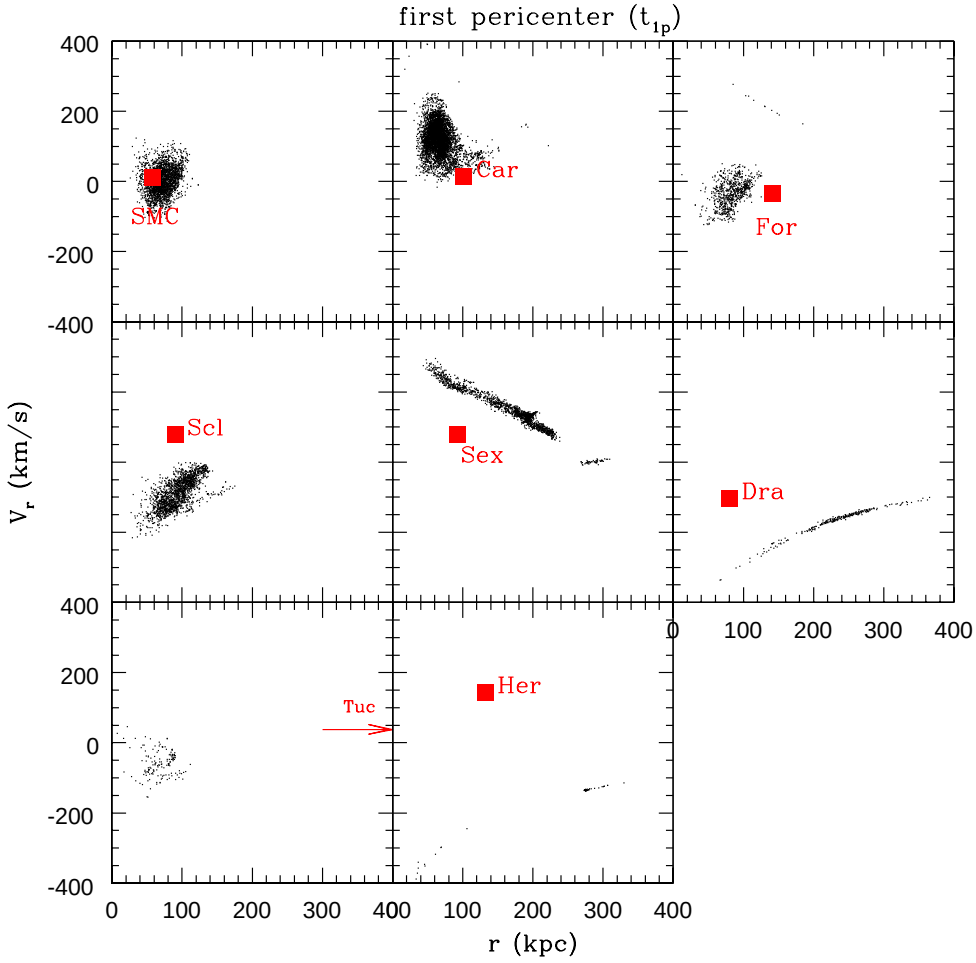

Figure 5. Galactocentric radial velocity and distance for dwarfs (filled squares) deemed possibly associated with the LMC according to the criterion of Fig. 4; i.e., $\delta_{50} < \delta_{\rm lim}$ at $t = t_{1p}$. Each panel also shows the r and V_r of all LMCa particles (dots) within a circle of radius $\delta_{\rm lim}$ centered at the position of each dwarf. This probes graphically whether the positional association indicated by proximity to the stream in the sky is corroborated by the velocity data. This test indicates that the SMC is the only known satellite clearly associated with the LMC if the Clouds are on their first pericentric approach. Aside from the SMC only Carina and Fornax seem marginally consistent with an LMC association. On the other hand, this test seems to rule out a possible association for all other candidates.

4 SUMMARY AND CONCLUSIONS

We use cosmological N-body simulations from the Aquarius Project to study the orbit of the LMC and its possible association with the SMC and other Milky Way satellites in light of new proper motion data (Kallivayalil et al. 2006; Piatek et al. 2008). We search the simulations for LMC dynamical analogs; i.e., accreted subhalos with pericentric distance (~ 50 kpc) and velocity (~ 400 km/s) matching those of the Clouds.

One suitable candidate (LMCa) is a $3.6 \times 10^{10} M_\odot$ system accreted at $z \sim 0.5$ ($t = 8.7$ Gyr) by Aq-A, a halo that, at $z = 0$ has a virial mass of $1.8 \times 10^{12} M_\odot$. LMCa turns around from a distance of 480 kpc at $t_{\rm ta} \sim 5$ Gyr ($z = 1.3$), accretes into the Milky Way halo at $t = 8.6$ Gyr ($z = 0.5$), and completes two pericentric passages by $z = 0$.

We use the positions and velocities of particles belonging to LMCa before infall in order to trace the orbital evolution of LMC-associated satellites and to inform the analysis of the likelihood that other Milky Way satellites were accreted in association with the Magellanic Clouds. Our main conclusions may be summarized as follows.

Near each pericentric passage the kinematic properties of LMCa match approximately those of the LMC. This implies that (i) the orbit of the LMC is not particularly unusual given the halo virial mass, and that (ii) it is difficult to decide, using only kinematical data, whether the LMC is on first approach or has already completed a full orbit.

If the LMC is *on first approach*, then most of its associated subhalos should be tightly clustered around its location. Although rare, some LMC-associated systems may still be found well away from the LMC but along the orbital path of the group. Since none of them has completed a single orbit there are strong position- radial velocity correlations that may be used to identify which satellites might have been accreted together with the LMC.

Of the known Milky Way satellites only the SMC is clearly associated with the LMC. A case can also be made for Fornax, Carina, and Sculptor, but it is not a particularly compelling one. This is particularly true when considering available proper motion

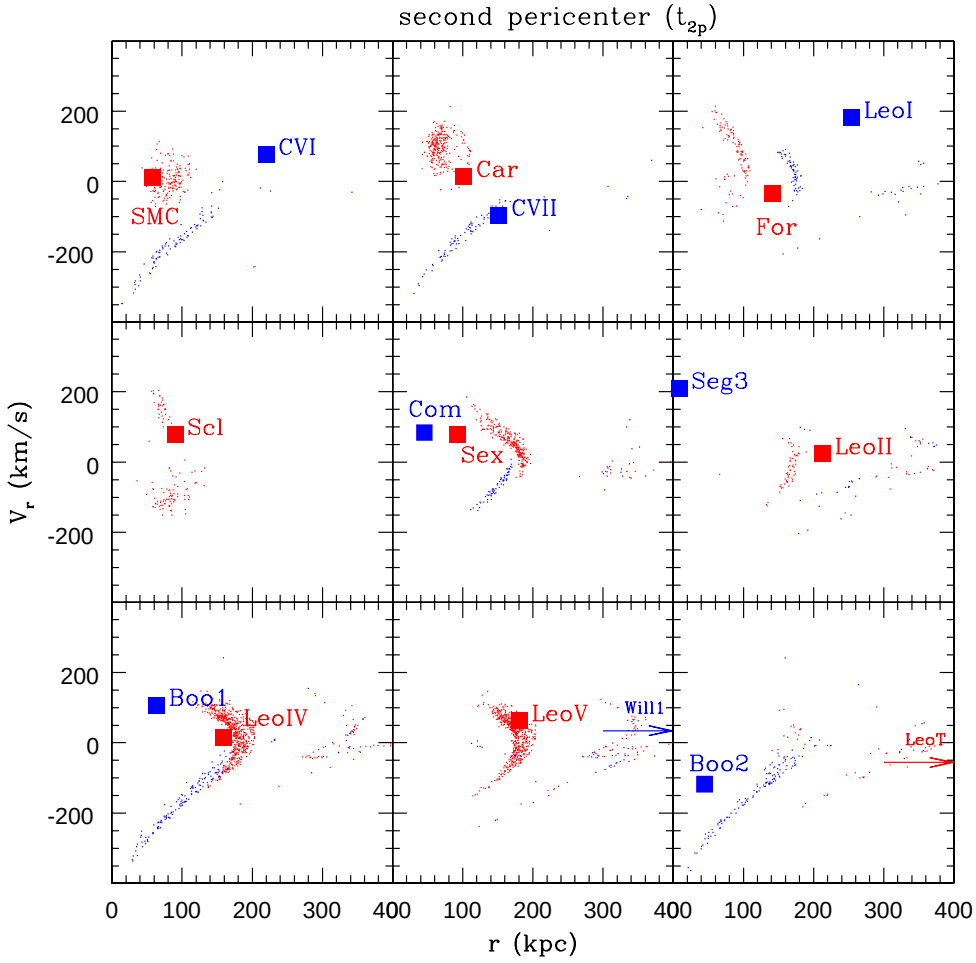

Figure 6. Same as Fig. 5 but for the second pericenter passage. Because the stream covers a wider area in the sky, the number of candidate dwarfs increases. We show *two* dwarfs per panel; arrows indicate systems that lie beyond the plotted region. In each panel red (blue) dots are stream particles in the $\delta_{\rm lim}$ circle around the dwarf indicated by a red (blue) square. This exercise confirms the association of the SMC, and suggests that several other dwarfs have kinematics consistent with association with the LMC. See text for further discussion.

data, which suggest that the orbital planes of these three satellites are not aligned with that of the Clouds.

If the LMC is near its *second pericenter* then several further dwarfs qualify for association. Leo II, Leo IV and Leo V, in particular, show strong spatial and velocity coincidence with the tidal debris from LMCa, making them prime candidates for past association with the LMC. Persuasive, but hardly conclusive, cases can also be made for a handful of other dwarfs, such as Canes Venatici II and Leo I. These tentative associations may be firmed up or refuted using the full spatial velocity, for which our simulations make a strong prediction: it must be such that the direction of the orbital angular momentum should point unambiguously in the anti-Galactic center direction.

We expect then few, if any, known Milky Way satellites to be associated with the Clouds, especially if they are on *first approach*. The simulations, however, make a very clear prediction in that case: most satellites associated with the Clouds have yet to disperse and should therefore be very near them. How many could we expect? The number depends strongly on the virial mass of the Clouds and is, therefore, highly uncertain. If the mass is as high as $1.3 \times 10^{11} M_{\odot}$, as suggested by the abundance-matching analysis of Boylan-Kolchin et al. (2010), then we would expect it to have of order 7 subhalos with peak circular velocities exceeding 20 km/s (Springel et al. 2008). This, according to the recent model of Font et al. (2011), is the minimum halo potential depth required to host a luminous dwarf.

Although the numbers seem modest, one may be encouraged by the fact that the LMC does have at least one companion (the SMC), so the possibility that they are part of a larger "Magellanic Galaxy" should not be dismissed too quickly. The surroundings of the Clouds might be hiding a trove of new Milky Way satellites awaiting discovery.

ACKNOWLEDGEMENTS

We would like to thank Volker Springel and Adrian Jenkins for their important contributions to the simulations in which this work is based on. The simulations for the Aquarius Project were carried out at the Leibniz Computing Centre, Garching, Germany, at

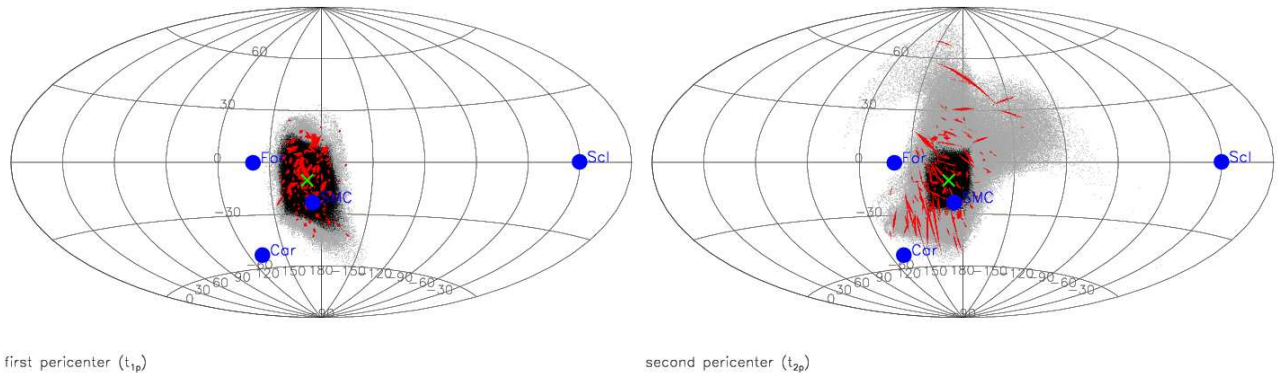

Figure 7. Direction of the orbital angular momentum of LMCa at first and second pericenter passages, compared with those of dwarfs with published proper motions. The directions are shown in an Aitoff projection of Galactic coordinates (l and b). The color coding is the same as in Figs. 2 and 3. All satellites associated with the LMC before infall are expected to have their orbital poles in a well defined region of the sky centered approximately at $(l, b) \sim (170°, -10°)$. Of the 4 dwarfs with measured full spatial motions only the SMC seems obviously associated with the LMC.

the Computing Centre of the Max-Planck-Society in Garching, at the Institute for Computational Cosmology in Durham, and on the STELLA supercomputer of the LOFAR experiment at the University of Groningen.

REFERENCES

Battaglia G., Helmi A., Morrison H., Harding P., Olszewski E. W., Mateo M., Freeman K. C., Norris J., Shectman S. A., 2005, MNRAS, 364, 433
Belokurov V., Walker M. G., Evans N. W., Faria D. C., Gilmore G., Irwin M. J., Koposov S., Mateo M., Olszewski E., Zucker D. B., 2008, ApJL, 686, L83
Belokurov V., Walker M. G., Evans N. W., Gilmore G., Irwin M. J., Mateo M., Mayer L., Olszewski E., Bechtold J., Pickering T., 2009, MNRAS, 397, 1748
Besla G., Kallivayalil N., Hernquist L., Robertson B., Cox T. J., van der Marel R. P., Alcock C., 2007, ApJ, 668, 949
Besla G., Kallivayalil N., Hernquist L., van der Marel R. P., Cox T. J., Kereš D., 2010, ApJL, 721, L97
Boylan-Kolchin M., Besla G., Hernquist L., 2010, ArXiv e-prints
Boylan-Kolchin M., Springel V., White S. D. M., Jenkins A., Lemson G., 2009, MNRAS, 398, 1150
Busha M. T., Wechsler R. H., Behroozi P. S., Gerke B. F., Klypin A. A., Primack J. R., 2010, ArXiv e-prints
Davis M., Efstathiou G., Frenk C. S., White S. D. M., 1985, ApJ, 292, 371
D'Onghia E., Lake G., 2008, ApJL, 686, L61
Font A. S., Benson A. J., Bower R. G., Frenk C. F., Cooper A. P., De Lucia G., Helly J. C., Helmi A., Li Y., McCarthy I. G., Navarro J. F., Springel V., Starkenburg E., Wang J., 2011, ArXiv e-prints
Gardiner L. T., Sawa T., Fujimoto M., 1994, MNRAS, 266, 567
Gnedin O. Y., Brown W. R., Geller M. J., Kenyon S. J., 2010, ArXiv e-prints
Guo Q., Cole S., Eke V., Frenk C., 2011, ArXiv e-prints
Kallivayalil N., van der Marel R. P., Alcock C., Axelrod T., Cook K. H., Drake A. J., Geha M., 2006, ApJ, 638, 772
Klimentowski J., Łokas E. L., Knebe A., Gottlöber S., Martinez-Vaquero L. A., Yepes G., Hoffman Y., 2010, MNRAS, 402, 1899
Klypin A., Zhao H., Somerville R. S., 2002, ApJ, 573, 597
Koch A., Wilkinson M. I., Kleyna J. T., Irwin M., Zucker D. B., Belokurov V., Gilmore G. F., Fellhauer M., Evans N. W., 2009, ApJ, 690, 453
Li Y., Helmi A., 2008, MNRAS, 385, 1365
Li Y., White S. D. M., 2008, MNRAS, 384, 1459
Lin D. N. C., Lynden-Bell D., 1982, MNRAS, 198, 707
Liu L., Gerke B. F., Wechsler R. H., Behroozi P. S., Busha M. T., 2010, ArXiv e-prints
Ludlow A. D., Navarro J. F., Springel V., Jenkins A., Frenk C. S., Helmi A., 2009, ApJ, 692, 931
Lynden-Bell D., 1976, MNRAS, 174, 695
Lynden-Bell D., 1982, The Observatory, 102, 7
Lynden-Bell D., Lynden-Bell R. M., 1995, MNRAS, 275, 429
Murai T., Fujimoto M., 1980, PASJ, 32, 581
Navarro J. F., Frenk C. S., White S. D. M., 1996, ApJ, 462, 563
Navarro J. F., Frenk C. S., White S. D. M., 1997, ApJ, 490, 493
Navarro J. F., Ludlow A., Springel V., Wang J., Vogelsberger M., White S. D. M., Jenkins A., Frenk C. S., Helmi A., 2010, MNRAS, 402, 21
Nidever D. L., Majewski S. R., Butler Burton W., Nigra L., 2010, ApJ, 723, 1618
Niederste-Ostholt M., Belokurov V., Evans N. W., Gilmore G., Wyse R. F. G., Norris J. E., 2009, MNRAS, 398, 1771
Piatek S., Pryor C., Bristow P., Olszewski E. W., Harris H. C., Mateo M., Minniti D., Tinney C. G., 2006, AJ, 131, 1445
Piatek S., Pryor C., Bristow P., Olszewski E. W., Harris H. C., Mateo M., Minniti D., Tinney C. G., 2007, AJ, 133, 818
Piatek S., Pryor C., Olszewski E. W., 2008, AJ, 135, 1024
Piatek S., Pryor C., Olszewski E. W., Harris H. C., Mateo M., Minniti D., Tinney C. G., 2003, AJ, 126, 2346
Power C., Navarro J. F., Jenkins A., Frenk C. S., White S. D. M., Springel V., Stadel J., Quinn T., 2003, MNRAS, 338, 14
Reid M. J., Menten K. M., Zheng X. W., Brunthaler A., Moscadelli L., Xu Y., Zhang B., Sato M., Honma M., Hirota T., Hachisuka K., Choi Y. K., Moellenbrock G. A., Bartkiewicz A., 2009, ApJ, 700, 137
Sales L. V., Navarro J. F., Abadi M. G., Steinmetz M., 2007a,

Table 1. Cartesian components of the unit vector that characterizes the direction of the (average) angular momentum of LMCa particles near each candidate LMC-associated satellite, according to the discussion of Fig. 5 and Fig. 6. For each dwarf, first and second rows list values at $t = t_{1p}$ and $t = t_{2p}$, respectively. Note that, because of the nearly polar orbit of LMCa, the angular momentum points in all cases in the $-X$ direction, i.e., to the Sun from the Galactic center. The angular momentum direction is also listed for satellites with published proper motions (third row), and may be used to assess their possible association with the Clouds.

Name	time	j_X	j_Y	j_Z
LMC	$t = t_{1p}$	-0.97 ± 0.03	0.14 ± 0.07	-0.19 ± 0.10
	$t = t_{2p}$	-0.97 ± 0.03	0.14 ± 0.06	-0.18 ± 0.09
	obs	-0.97 ± 0.01	0.14 ± 0.02	-0.18 ± 0.03
SMC	$t = t_{1p}$	-0.92 ± 0.05	0.04 ± 0.10	-0.35 ± 0.08
	$t = t_{2p}$	-0.90 ± 0.05	0.05 ± 0.17	-0.38 ± 0.10
	obs	-0.91 ± 0.05	0.08 ± 0.11	-0.39 ± 0.09
Carina	$t = t_{1p}$	-0.93 ± 0.12	0.25 ± 0.07	-0.04 ± 0.20
	$t = t_{2p}$	-0.95 ± 0.03	0.25 ± 0.06	-0.01 ± 0.15
	obs	-0.40 ± 0.48	0.46 ± 0.18	-0.79 ± 0.38
Fornax	$t = t_{1p}$	-0.92 ± 0.20	0.19 ± 0.11	0.20 ± 0.07
	$t = t_{2p}$	–	–	–
	obs	-0.77 ± 0.04	0.63 ± 0.05	0.00 ± 0.03
Sculptor	$t = t_{1p}$	–	–	–
	$t = t_{2p}$	-0.94 ± 0.06	0.00 ± 0.41	0.04 ± 0.05
	obs	0.86 ± 0.03	-0.50 ± 0.04	0.003 ± 0.005
Canes Venatici II	$t = t_{1p}$	–	–	–
	$t = t_{2p}$	-0.92 ± 0.10	-0.28 ± 0.26	-0.06 ± 0.07
Leo II	$t = t_{1p}$	–	–	–
	$t = t_{2p}$	-0.92 ± 0.05	0.21 ± 0.21	-0.28 ± 0.15
Leo IV	$t = t_{1p}$	–	–	–
	$t = t_{2p}$	-0.98 ± 0.02	0.16 ± 0.12	-0.01 ± 0.09
Leo V	$t = t_{1p}$	–	–	–
	$t = t_{2p}$	-0.97 ± 0.02	0.17 ± 0.13	-0.03 ± 0.09

MNRAS, 379, 1475
Sales L. V., Navarro J. F., Abadi M. G., Steinmetz M., 2007b, MNRAS, 379, 1464
Shattow G., Loeb A., 2009, MNRAS, 392, L21
Smith M. C., et al. 2007, MNRAS, 379, 755
Spergel D. N., Verde L., Peiris H. V., Komatsu E., Nolta M. R., Bennett C. L., Halpern M., Hinshaw G., Jarosik N., Kogut A., Limon M., Meyer S. S., Page L., Tucker G. S., Weiland J. L., Wollack E., Wright E. L., 2003, ApJS, 148, 175
Springel V., Wang J., Vogelsberger M., Ludlow A., Jenkins A., Helmi A., Navarro J. F., Frenk C. S., White S. D. M., 2008, MNRAS, 391, 1685
Springel V., White S. D. M., Frenk C. S., Navarro J. F., Jenkins A., Vogelsberger M., Wang J., Ludlow A., Helmi A., 2008, Nature, 456, 73
Springel V., Yoshida N., White S. D. M., 2001, New Astronomy, 6, 79
van der Marel R. P., Alves D. R., Hardy E., Suntzeff N. B., 2002, AJ, 124, 2639
Xue X. X., Rix H. W., Zhao G., Re Fiorentin P., Naab T., Steinmetz M., van den Bosch F. C., Beers T. C., Lee Y. S., Bell E. F., Rockosi C., Yanny B., Newberg H., Wilhelm R., Kang X., Smith M. C., Schneider D. P., 2008, ApJ, 684, 1143